

Entropy Control of the Cross-Reaction between Carbon-Centered and Nitroxide Radicals

Jens Sobek, Rainer Martschke, and Hanns Fischer*

Contribution from the Physikalisch-Chemisches Institut der Universität Zürich, Winterthurerstrasse 190, CH-8057 Zürich, Switzerland

Received October 10, 2000

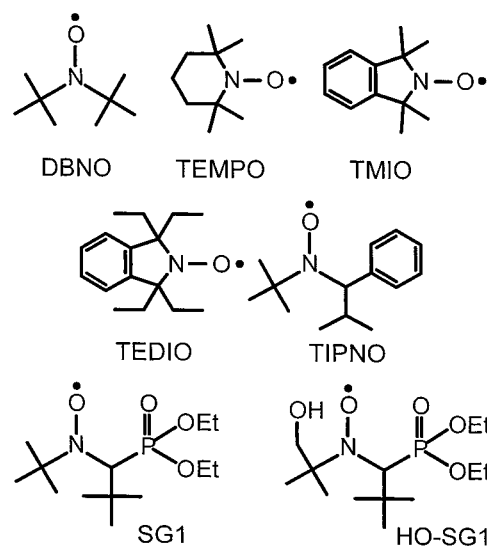
Abstract: Absolute rate constants for the cross-coupling reaction of several carbon-centered radicals with various nitroxides and their temperature dependence have been determined in liquids by kinetic absorption spectroscopy. The rate constants range from $<2 \times 10^5 \text{ M}^{-1} \text{ s}^{-1}$ to $2.3 \times 10^9 \text{ M}^{-1} \text{ s}^{-1}$ and depend strongly on the structure of the nitroxide and the carbon-centered radical. Grossly, they decrease with increasing rate constant of the cleavage of the corresponding alkoxyamine. In many cases, the temperature dependence shows a non-Arrhenius behavior. A model assuming a short-lived intermediate that is hindered to form the coupling product by an unfavorable activation entropy leads to a satisfactory analytic description. However, the behavior is more likely due to a barrierless single-step reaction with a low exothermicity where the free energy of activation is dominated by a large negative entropy term.

Introduction

In mechanistic studies, stable nitroxide radicals are widely used as scavengers for carbon-centered radicals (cf. Schemes 1, 2). Therefore, the rates of the cross-reaction between these species have been of much interest. For a series of alkyl radicals reacting with various nitroxides, Beckwith and Ingold et al.^{1–4} observed rate constants at room temperature. They are considerably smaller than those that are diffusion controlled and decrease with increasing radical stabilization and steric demand of substituents, both of the nitroxide and the carbon-centered species. Modest solvent effects were also found to prefer reactions in non polar and less viscous media. Furthermore, for a few cases, the temperature dependence of the rate constants was measured. It is remarkably weak and shows activation energies close to zero and unusually small pre-exponential factors. Hence, the small rate constants are not due to large barriers, but are instead caused by unfavorable negative activation entropies.^{3,4}

Since the first publications of Rizzardo et al.⁵ and Georges et al.⁶ on the application of nitroxides as mediators of controlled living radical polymerizations, the cross-coupling of nitroxides and carbon-centered propagating radicals has gained additional attention. Together with the rate constant for the reverse reaction and the cleavage reaction of “dormant” polymeric alkoxyamines (k_d), the cross-coupling rate constant (k_c) determines the polymerization time, the degree of livingness, and the polydispersity index (PDI), that is, the quality of the living polymer.

Scheme 1



In particular, the polymerization time decreases and the livingness increases with increasing ratio k_d/k_c , that is, the equilibrium constant of the reversible cleavage; whereas, the PDI decreases with increasing product $k_d k_c$. Therefore, k_d and k_c must fall into quite limited ranges to ensure the production of living and narrowly dispersed polymers in reasonable times.^{7,8} In particular, predictions of the course of polymerizations require knowledge and understanding of the reaction kinetics.

The cleavage rates of alkoxyamines (k_d) were investigated in some detail for both polymeric^{8–11} and low-molecular-

(7) Fischer, H. *Macromolecules* **1997**, *30*, 5666. Fischer, H. *J. Polym. Sci. A: Polym. Chem.* **1999**, *37*, 1885.

(8) Souaille, M.; Fischer, H. *Macromolecules* **2000**, *33*, 7378.

(9) Goto, A.; Terauchi, T.; Fukuda, T.; Miyamoto, T. *Macromol. Rapid Commun.* **1997**, *18*, 673. Goto, A.; Fukuda, T. *Macromolecules* **1999**, *32*, 618. Fukuda, T.; Goto, A.; Ohno, K. *Macromol. Rapid Commun.* **2000**, *21*, 151.

(10) Bon, S. A. F.; Chambard, G.; German, A. L. *Macromolecules* **1999**, *32*, 8269.

* Fax: +41-1-635 68 56. E-mail: hfischer@pci.unizh.ch.

(1) Beckwith, A. L. J.; Bowry, V. W.; Ingold, K. U. *J. Am. Chem. Soc.* **1992**, *114*, 4983.

(2) Bowry, V. W.; Ingold, K. U. *J. Am. Chem. Soc.* **1992**, *114*, 4992.

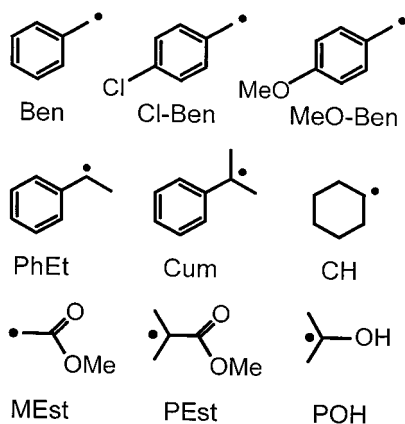
(3) Chateaufneuf, J.; Luszyk, J.; Ingold, K. U. *J. Org. Chem.* **1988**, *53*, 1629.

(4) Beckwith, A. L. J.; Bowry, V. W.; Moad, G. *J. Org. Chem.* **1988**, *53*, 1632.

(5) Solomon, D. H.; Rizzardo, E.; Cacioli, P. U.S. Patent 4581429; *Chem. Abstr.* **1985**, *102*, 221335q.

(6) Georges, M. K.; Veregim, R. P. N.; Kazmaier, P. M.; Hamer, G. K. *Macromolecules* **1993**, *26*, 2987.

Scheme 2



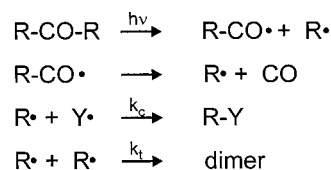
model^{12–22} systems in wide temperature ranges, and predictive rationalizations have been offered.^{20,21} In comparison, despite the pioneering work,^{1–4} much less is known about k_c and, in particular, for the cross-reaction of such nitroxides and carbon-centered radicals which constitute reasonable models for polymerizations.^{11,13,14,19,22,23} In addition, a wider knowledge and a better understanding of the unusual temperature dependence of the cross-reaction rates is needed, because the polymerizations are normally carried out at elevated temperatures of 80–120 °C.

In continuation of our earlier work,^{19,22} we have now studied the kinetics of the cross-reaction between the technically relevant nitroxides of Scheme 1 and the carbon-centered radicals of Scheme 2 in a fairly large temperature range by kinetic absorption spectroscopy. Not unexpectedly in view of the earlier results,^{1–4} we find for most cases a non-Arrhenius behavior of the rate constants and discuss this in terms of appropriate models for entropy control.

Experimental Section

Materials and Solvents. Acetonitrile (ACN), cyclohexane (CHN), 2,2,4-trimethylpentane (TMP), 1,1-diphenylethene (DPE), and dibenzyl ketone were received from Fluka and dimethylacetonedicarboxylate from Lancaster Synthesis in the purest available forms and were used as received. *tert*-Butylbenzene (tBB, Fluka) was distilled once; di-*tert*-butylperoxide (Schuchardt) was distilled twice before use. DBNO (Aldrich) was purified by column chromatography. TEMPO (Aldrich) was sublimed and found to be 97% pure by titration. 2,4-Dihydroxy-

Scheme 3



2,4-dimethylpentane-3-one,²⁴ α,α' -dimethyl-dibenzyl ketone, $\alpha,\alpha,\alpha',\alpha'$ -tetramethyl-dibenzyl ketone, 2,2',4,4'-tetramethyl-dimethyl acetonedicarboxylate, 1,3-bis(4-chlorobenzyl)propan-2-one, and 1,3-bis(4-methoxybenzyl)propan-2-one²⁵ were synthesized according to standard procedures. Tetramethyl-isoinindolin-1-oxyl (TMIO) and tetraethyl-isoinindolin-1-oxyl (TEDIO) were provided by Ciba Specialty Chemicals (Basel). 2,2,5,5-Tetramethyl-4-phenyl-3-azahexane-3-oxyl (TIPNO), *N,N*-(1,1-dimethylethyl-1)-(1-diethyl-phosphono-2,2-dimethyl-propyl-1)-*N*-oxyl (DEPN, SG1), and *N,N*-(1,1-(hydroxymethyl)-methyl-ethyl-1)-(1-diethylphosphono-2,2-dimethyl-propyl-1)-*N*-oxyl (HO-SG1), were obtained from Prof. P. Tordo (Marseille).

Time-Resolved Absorption Measurements. The experimental setup for kinetic absorption spectroscopy has been described.^{26–28} Apart from cyclohexyl, the carbon-centered radicals of Scheme 2 were produced from the corresponding symmetrically substituted ketones by laser pulse (20-ns) excitation at $\lambda_{\text{exc}} = 308$ nm, which initiates the reactions of Scheme 3. For high enough temperatures, the decarbonylation of the acyl radicals is sufficiently fast^{27–30} so that other reactions of these species can be ignored. Cyclohexyl radicals were produced by hydrogen atom abstraction from cyclohexane by *tert*-butyloxy radicals generated by pulse photolysis of di-*tert*-butyl peroxide (20 vol % in CHN).

In typical experimental series aimed at the cross-reaction constants, kinetic traces were monitored for solutions containing 2–3 mM ketone and at least three different nitroxide concentrations in the range of 0.12–70 mM. To measure the self-termination rate constants of the carbon-centered radicals, 20 mM ketone solutions were used. It was checked in each case that the results did not depend on the laser intensity. Solutions were freed from oxygen prior to use by 30 min of purging with argon. Temperatures given are exact to ± 1 K. Because of the weak temperature dependence of most of the cross-reaction rate constants, the temperature dependence of the nitroxide concentration was taken into consideration in the analysis. For the solvent tBB, the temperature range of observation was limited by the freezing point and the rate of decarbonylation of the acyl radical precursor (Scheme 3) to greater than -30 °C for tertiary and secondary radicals and to greater than -5 °C for primary radicals. Unfortunately, the rate constants of MEst and PEst could not be measured in this solvent because, as evidenced by ESR experiments, the precursor ketone is photoreduced by tBB. However, in ACN, the desired radicals are cleanly produced between -30 °C and 60 °C. Errors of rate constants are given in units of the last quoted digit.

Analysis. For carbon-centered radicals with sufficiently high decadic molar absorbances at wavelengths larger than ~ 315 nm, their kinetic traces post flash were followed directly. Absorbance spectra and absorption coefficients were determined following ref 27 for Ben ($\epsilon = 7000 \pm 2000 \text{ M}^{-1} \text{ s}^{-1}$ at $\lambda_{\text{max}} = 316$ nm in tBB),^{27,31,32} PhEt ($\epsilon = 5000 \pm 2000$ at $\lambda_{\text{max}} = 320$ nm in tBB),^{33,34} and Cum ($\epsilon = 4500 \pm 1500$

(11) Benoit, D.; Grimaldi, S.; Robin, S.; Finet, J.-P.; Tordo, P.; Gnanou, Y. *J. Am. Chem. Soc.* **2000**, *122*, 5929.

(12) Kovtun, G. A.; Aleksandrov, A. L.; Golubev, V. A. *Bull. Acad. Chim. U.S.S.R., Div. Chem.* **1974**, *10*, 2115.

(13) (a) Howard, J. A.; Tait, J. C. *J. Org. Chem.* **1978**, *43*, 4279. (b) Grattan, D. W.; Carlsson, D. J.; Howard, J. A.; Wiles, D. M. *Can. J. Chem.* **1979**, *57*, 2834.

(14) Arends, I. W. C. E.; Mulder, P.; Clark, K. B.; Wayner, D. D. M. *J. Phys. Chem.* **1995**, *99*, 8182.

(15) Moad, G.; Rizzardo, E. *Macromolecules* **1995**, *28*, 8722.

(16) Skene, W. G.; Belt, S. T.; Connolly, T. J.; Hahn, P.; Scaiano, J. C. *Macromolecules* **1998**, *31*, 9103.

(17) Ciriano, M. V.; Korth, H. G.; van Scheppingen, W. B.; Mulder, P. *J. Am. Chem. Soc.* **1999**, *121*, 6375.

(18) Connolly, T. J.; Baldovi, M. V.; Mohtat, N.; Scaiano, J. C. *Tetrahedron Lett.* **1996**, *37*, 4919.

(19) LeMercier, C.; LeMoigne, F.; Tordo, P.; Lutz, J.-F.; Lacroix-Desmazes, P.; Boutevin, B.; Couturier, J.-L.; Guerret, O.; Marque, S.; Martschke, R.; Sobek, J.; Fischer, H. *ACS Symp. Ser.* **2000**, *768*, 108.

(20) Marque, S.; LeMercier, C.; Tordo, P.; Fischer, H. *Macromolecules* **2000**, *33*, 4403.

(21) Marque, S.; Fischer, H.; Baier, E.; Studer, A. *J. Org. Chem.*, in press. Marque, S.; Fischer, H., to be published.

(22) Kothe, T.; Marque, S.; Martschke, R.; Popov, M.; Fischer, H. *J. Chem. Soc., Perkin Trans. 2* **1998**, 1553.

(23) Skene, W. G.; Scaiano, J. C.; Listigovers, N. A.; Kazmaier, P. M.; Georges, M. K. *Macromolecules* **2000**, *33*, 5065.

(24) Faworsky, F.; Umnova, A. *J. Prakt. Chem. II* **1912**, *88*, 679.

(25) Claridge, R. F. C.; Fischer, H. *J. Phys. Chem.* **1983**, *87*, 1960.

(26) Martschke, R.; Farley, R. D.; Fischer, H. *Helv. Chim. Acta* **1997**, *80*, 1363. Martschke, R.; Ph.D. Thesis, University of Zurich, 1999.

(27) Tsentralovich, Y. P.; Fischer, H. *J. Chem. Soc., Perkin Trans. 2* **1994**, 729.

(28) Salzmann, M.; Tsentralovich, Y. P.; Fischer, H. *J. Chem. Soc., Perkin Trans. 2* **1994**, 2119.

(29) Turro, N. J.; Gould, I. R.; Baretz, B. H. *J. Phys. Chem.* **1983**, *87*, 531.

(30) Hany, R.; Fischer, H. *Chem. Phys.* **1993**, *172*, 131.

(31) Zimmt, M. B.; Doubleday, C.; Turro, N. J. *J. Am. Chem. Soc.* **1986**, *108*, 3618.

(32) Tanimoto, Y.; Takashima, M.; Itoh, M. *Bull. Chem. Soc. Jpn.* **1989**, *62*, 39.

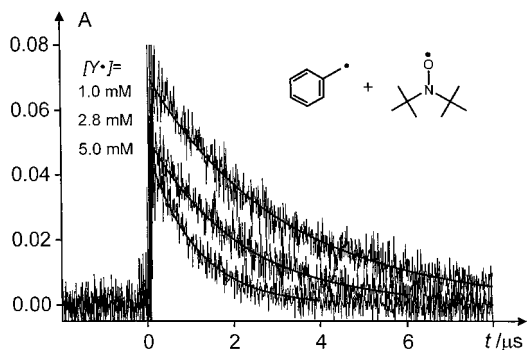


Figure 1. Time dependence of the benzyl absorption at 316 nm in *tert*-butylbenzene for 297 K and various DBNO concentrations.

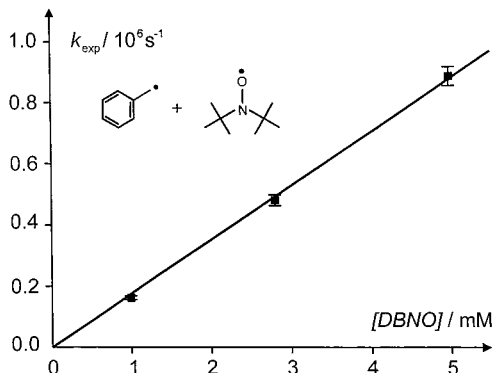


Figure 2. Concentration dependence of the apparent rate constant for the cross-coupling of benzyl with DBNO in *tert*-butylbenzene for 297 K.

$M^{-1} s^{-1}$ at $\lambda_{\max} = 321$ nm in ACN and at $\lambda_{\max} = 323$ nm in tBB, respectively).^{35,36} Those of Cl-Ben ($\epsilon = 7200 \pm 150 M^{-1} s^{-1}$ at $\lambda_{\max} = 317$ nm in CHN) and MeO-Ben ($\epsilon = 2900 \pm 300 M^{-1} s^{-1}$ at $\lambda_{\max} = 321$ nm in CHN) are known from modulation spectroscopy.²⁵ The absorption coefficient of PEst ($\epsilon = 440 M^{-1} s^{-1}$ at $\lambda = 320$ nm in ACN) was taken from ref 37.

Figure 1 shows a typical absorbance decay of a carbon-centered radical. The rate equation is

$$\frac{d[R\cdot]}{dt} = -2k_t[R\cdot]^2 - k_{\text{exp}}[R\cdot] \quad (1)$$

with $k_{\text{exp}} = k_c[Y\cdot]$. The nitroxide concentration $[Y\cdot]$ is constant, because it is much larger than the concentration of the carbon-centered radicals $[R\cdot]$. Equation 1 is easily integrated and yields the change in optical density produced by $R\cdot$.

$$\frac{A(t)}{d} = \frac{k_{\text{exp}}}{2k_t \left[\left(1 + \frac{k_{\text{exp}} d}{2k_t \epsilon A_0} \right) e^{k_{\text{exp}} t} - 1 \right]} \quad (2)$$

For $k_{\text{exp}} = 0$, eq 2 reduces to a pure second-order decay of the absorbance of $R\cdot$, and this was applied to extract $2k_t/\epsilon$ and the self-termination rate constants $2k_t$ from kinetic profiles that were obtained with nitroxide-free solutions. For $[Y\cdot] \neq 0$, eq 2 was fitted to the data (Figure 1) to obtain A_0 and k_{exp} . Variation of $[Y\cdot]$ and plotting k_{exp} vs $[Y\cdot]$ then yielded k_c as shown in Figure 2.

The absorbance of the radicals MEst, POH, and CH is too weak at $\lambda \geq 315$ nm and could not be followed directly. Therefore, the cross-reaction was followed in competition to the radical addition to 1,1-

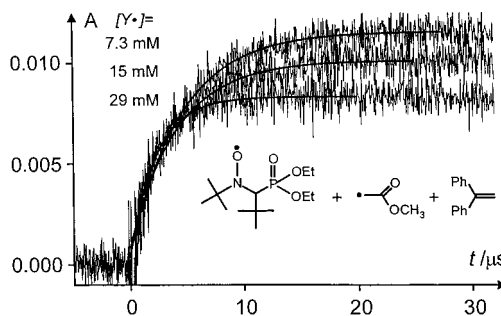


Figure 3. Time dependence of the absorption of the adduct of the methoxycarbonylmethyl radical to 1,1-diphenylethene at 334 nm in acetonitrile for 297 K and various SG1 concentrations.

diphenylethene, and the absorbance of the adduct radical (3) was monitored at 334 nm.²⁶



For sufficiently low radical concentrations, the kinetic traces reached a plateau with constant absorbance at longer times, indicating that the self-termination of the adduct radical can be neglected on the experimental time scale. This plateau also rules out a fast reaction between the adduct radical and the nitroxide. In fact, Howard et al.^{13a} estimated the rate constant for the coupling of the 1,1-diphenylethyl radical with 4-oxo-TEMPO as low as $k_c = 5 \times 10^4 M^{-1} s^{-1}$ at 30 °C. Figure 3 shows absorbance changes for several nitroxide concentrations that were observed with the competition technique.

Neglecting all self-terminations, the possible cross-termination between the primary carbon-centered radical $R\cdot$ and its DPE adduct and the cross-reaction between adduct and nitroxide yields the relevant rate equations

$$\frac{d[R\cdot]}{dt} = -(k_c[Y\cdot] + k_M[\text{DPE}])[R\cdot] = -k_{\text{exp}}[R\cdot] \quad (4)$$

$$\frac{d[R - \text{DPE}\cdot]}{dt} = k_M[\text{DPE}][R\cdot] \quad (5)$$

with k_{exp} now given by $k_{\text{exp}} = k_c[Y\cdot] + k_M[\text{DPE}]$. These provide the changes in optical density caused by $R\cdot$ and $R - \text{DPE}\cdot$.

$$\frac{A(t)}{d} = \left[\epsilon_R - \epsilon_{R - \text{DPE}} \frac{k_M[\text{DPE}]}{k_{\text{exp}}} \right] [R\cdot](t) + \epsilon_{R - \text{DPE}} \frac{k_M[\text{DPE}]}{k_{\text{exp}}} [R\cdot]_0 \quad (6)$$

and

$$\ln \left[\frac{A_\infty}{A_\infty - A(t)} \right] = \ln \left[\frac{1}{1 - \frac{\epsilon_R}{\epsilon_{R - \text{DPE}}} \frac{k_{\text{exp}}}{k_M[\text{DPE}]}} \right] + k_{\text{exp}} t \quad (7)$$

A_∞ is the absorbance at the plateau of the kinetic trace. Equation 7 was applied for analysis, and fits are included in Figure 3. The addition rate constant k_M was determined separately with solutions containing DPE but no nitroxide, and $[Y\cdot]$ was varied with $[\text{DPE}]$ fixed to obtain k_c . Figure 4 shows a plot of $k_{\text{exp}} - k_M[\text{DPE}]$ vs the nitroxide concentration. The reasonable linear dependence supports the approximations made in the derivation of eq 7.

Results and Discussion

Addition Rate Constants. The rate constants for the addition of MEst, POH and CH to DPE and their Arrhenius parameters are listed in Table 1. They agree reasonably well with earlier

(33) McAskill, N. A.; Sangster, D. F. *Aust. J. Chem.* **1984**, *37*, 2137.

(34) Brede, O.; Helmstret, W.; Mehnert, R. *J. Prakt. Chem.* **1974**, *316*, 402.

(35) Sumiyoshi, T.; Mikiharu, K.; Kuwae, Y.; Schnabel, W. *Bull. Chem. Soc. Jpn.* **1987**, *60*, 77.

(36) Faria, J. L.; Steenken, S. *J. Phys. Chem.* **1992**, *96*, 10869.

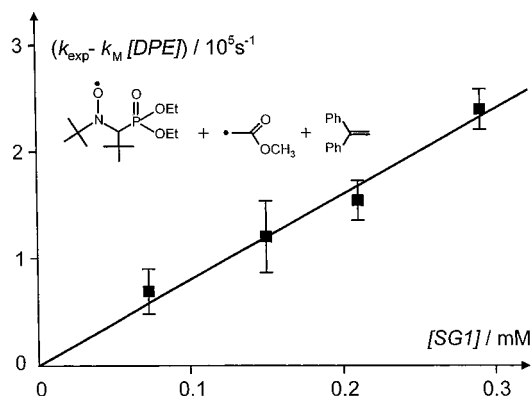


Figure 4. Concentration dependence of the apparent rate constant for the cross-coupling of methoxycarbonylmethyl with SG1 in acetonitrile for 297 K.

Table 1. Rate Constants and Arrhenius Parameters for the Addition of Carbon-Centered Radicals to 1,1-Diphenylethene^a

radical	solv	$k_M(297)$ $10^4 \text{ M}^{-1} \text{ s}^{-1}$	temp range K	E_a kJ mol^{-1}	$\log(A)$ $\text{M}^{-1} \text{ s}^{-1}$
MEst	ACN	870(11)	297		
POH	MeOH	71(2)	245–324	5.4(6)	6.9(2)
CH	CHN	9.2(4)	297–333	12.8(4)	7.2(1)

$$^a E_a/\text{kcal mol}^{-1} = E_a/\text{kJ mol}^{-1}/4.185$$

data for the same reactions, for example, for MEst, $k_M(297)^{38} = 1 \times 10^7 \text{ M}^{-1} \text{ s}^{-1}$, and for POH, $k_M(297)^{39} = 8.5 \times 10^5 \text{ M}^{-1} \text{ s}^{-1}$. They also are of the expected order of magnitude and deserve no further comment.

Self-Termination Rate Constants. Table 2 presents the self-termination rate constants of carbon-centered radical measured in this work. In all cases, the temperature dependence is well-described by the Arrhenius equation. There is good agreement with earlier literature,^{25,34,40,41} and small deviations are probably due to different solvents or the uncertainty of the absorption coefficients.

With the equations of Stokes–Einstein and von Smoluchowski and the known temperature dependence of the viscosity,^{26,42} one predicts the rate constants and Arrhenius parameters for diffusion-limited reactions⁴³ that are also compiled in Table 2. Comparison to the experimental data reveals that the self-termination of the carbon-centered radicals occurs close to the diffusion limit.

Cross-Reaction Rate Constants. For several nitroxide/radical pairs, the cross-reaction rate constants were measured over a considerable temperature range, and some experimental values are collected in Table 3. Also given are the rate constants at the technically important higher temperature of 120 °C or 393 K. These were obtained by extrapolation using eq 9, which is explained further below. The data range from $\leq 2 \times 10^5$ to $3 \times 10^9 \text{ M}^{-1} \text{ s}^{-1}$. Only for MEst and POH reacting with TEMPO, they are of the order of magnitude expected for diffusion control (cf. Table 2), and for all other systems they are considerably smaller. For a given nitroxide, less stabilized primary radicals

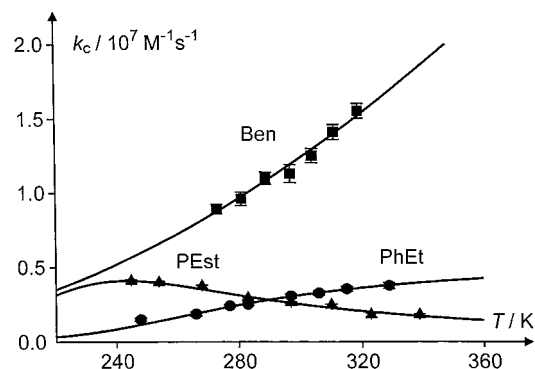


Figure 5. Temperature dependence of the cross-coupling rate constant of the carbon-centered radicals benzyl, 1-phenylethyl, and 2-methoxycarbonyl-2-propyl with SG1.

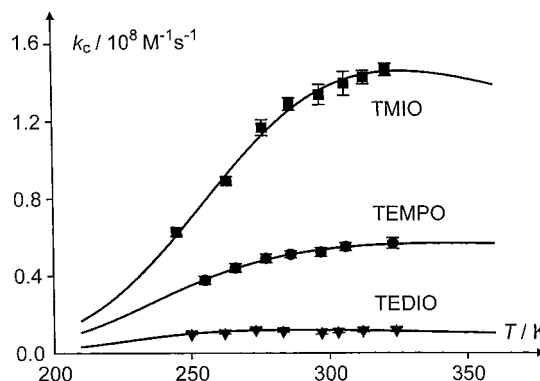


Figure 6. Temperature dependence of the cross-coupling rate constant of the cumyl radical with TMIO, TEMPO, and TEDIO.

(MEst) react faster than stabilized secondary and tertiary radicals (PhEt, PEst, Cum), and for the same or similar carbon-centered radicals the nitroxides show the reactivity pattern $\text{TMIO} > \text{TEMPO} > \text{DBNO} = \text{TEDIO} > \text{TIPNO} > \text{SG1} \cong \text{HO-SG1}$. These trends agree with previous experience and an interpretation of the smaller rate constants in terms of radical stabilization and steric factors hindering the reaction.^{1–4} There is also an excellent agreement with earlier room temperature data for CH, Ben, PhEt, or Cum reacting with TMIO, TEMPO, or DBNO,^{1–4,22,23} but not for PhEt + TEMPO in nonpolar solvent, where our rate constant is about 2.5 times larger than the previous value.¹

For comparison, the rate constants k_d of the cleavage of the corresponding alkoxyamines,^{20–23} are also given in Table 3. Grossly, k_d and k_c exhibit opposite substituent effects; that is, a faster cleavage of an alkoxyamine goes parallel with a slower radical cross-reaction. The cleavage is generally faster for the release of more stabilized and sterically congested radicals,^{20–23} and for SG1 and TEDIO the cross-reaction rate constants decrease in the same order. With the exception of PESt, this order is also obeyed for TEMPO. For similar carbon-centered radicals, the alkoxyamine cleavage rates increase in the order $\text{TMIO} < \text{TEMPO} < \text{TEDIO} = \text{TIPNO} = \text{SG1} < \text{DBNO}$, and this is also the reverse order of the cross-reaction constants, with the clear exception of DBNO. However, in detail, there is no simple relation between the cross-reaction and the cleavage rate constants k_c and k_d , because their variations with radical structures differ markedly. Thus, variation of the carbon-centered radical changes k_d both for TEMPO and SG1 by about 6 orders of magnitude. However, k_c varies by 3–4 orders of magnitude for SG1 and by only 2 orders of magnitude for TEMPO. Nevertheless, the opposite substituent effects on the rate constants point to similar factors of influence for both the

(37) Wojnárovits, L.; Takács, E. *Res. Chem. Intermed.* **1999**, *25*, 275.

(38) Wu, J. Q.; Beranek, I.; Fischer, H. *Helv. Chim. Acta* **1995**, *78*, 194. Beranek, I.; Fischer, H. In *Free Radicals in Synthesis and Biology*; Minisci, F., Ed.; Kluwer: Dordrecht, 1988.

(39) Batchelor, S. N.; Fischer, H. *J. Phys. Chem.* **1996**, *100*, 9794.

(40) Lehni, M.; Schuh, H.-H.; Fischer, H. *Int. J. Chem. Kinetics* **1979**, *11*, 705.

(41) Savitsky, A. N. Ph.D. Thesis, University of Zurich, 1998.

(42) Viswanath, D. S.; Natarajan, G. *Data Book on the Viscosity of Liquids*; Hemisphere Publishing Corporation: New York, 1989.

(43) Schuh, H.-H.; Fischer, H. *Helv. Chim. Acta* **1978**, *61*, 2130.

Table 2. Rate Constants and Arrhenius Parameters for the Self-Termination of Carbon-Centered Radicals^a

radical	solv.	$2k_t(297)/\epsilon \text{ } 10^5 \text{ cm}^2 \text{ s}^{-1}$	$2k_t(297)/10^9 \text{ M}^{-1} \text{ s}^{-1}$	temp range, K	$E_a/\text{kJ mol}^{-1}$	$\log(A/\text{M}^{-1} \text{ s}^{-1})$	data points
Ben	tBB	4.3(3)	3.0(3)	269–318	13.7(2)	11.9(5)	6
Cl–Ben	tBB	4.2(3)	3.0(3)	297–337	11.3(15)	11.6(2)	5
MeO–Ben	tBB	7.6(3)	2.2(3)	297–331	9.8(13)	11.0(3)	4
PhEt	tBB	3.8(1)	1.9(1)	261–330	12.2(4)	11.4(1)	7
Cum	tBB	2.7(2)	1.2(2)	240–325	13.4(3)	11.4(1)	9
D limit ^b	tBB		1.4	273–336	13.6(3)	11.6(1)	
PhEt	TMP	8.8(3)	4.4(3)	268–323	8.7(4)	11.2(1)	6
D limit ^b	TMP		3.4	273–323	11.4(2)	11.6(4)	
PEst	ACN	111(4)	4.4(4)	258–338	7.9(2)	11.1(1)	7
D limit ^b	ACN		4.4	280–360	10.3(1)	11.5(1)	

^a ($E_a/\text{Kcal Mol}^{-1} = E_a/\text{KJ Mol}^{-1}/4.185$) ^b Calculated from the temperature dependence of T/η with the von Smoluchowski–Stokes–Einstein approximation and a spin statistical factor of 0.25 with viscosity data from ref 42.

alkoxyamine cleavage and the cross-reaction, and this will be discussed later.

As mentioned above, only very few temperature dependencies of the cross-reaction rate constants were available, so far. They show rather weak variations, with activation energies close to zero and pre-exponential factors which are smaller than expected for a usual radical coupling reaction (cf. Table 2).^{3,4} For instance, Chateaufort et al.³ reported $\log(k_c/\text{M}^{-1} \text{ s}^{-1}) = 9.3(4) - 3.7(5)/2.3RT$ (kJ mol⁻¹) or $\log(k_c/\text{M}^{-1} \text{ s}^{-1}) = 9.3(4) - 0.9(1)/2.3RT$ (kcal mol⁻¹) for the reaction of Ben with TEMPO in TMP. Figures 5 and 6 show representative temperature dependencies found in this work. For SG1 reacting with Ben (Figure 5), the temperature dependence is described by the Arrhenius equation, and this holds also for POH reacting with TEMPO and for HO–SG1 with PhEt. The Arrhenius parameters for these rate constants are given in Table 4. For POH + TEMPO, the frequency factor and the activation energy are compatible with a diffusion-limited process (cf. Table 2), whereas for the two other reactions, the frequency factors are too low.

For most of the remaining cross-reactions, the rate constants cannot be described by the Arrhenius equation. They increase with increasing temperature at low temperatures and then attain or approach limiting values as exemplified in Figure 5 for PhEt reacting with SG1 and in Figure 6 for Cum reacting with three different nitroxides.⁴⁴ For the reaction of PEst with SG1, a decrease of the rate constants with increasing temperature is observed (Figure 5); that is, the apparent activation energy is negative.

A discussion of the temperature dependencies requires the knowledge of the nature of the cross-reaction, because different mechanisms in different temperature ranges may lead to unusual behavior. The reaction is often assumed to be by coupling only. This is very reasonable for the primary benzyl-type radicals and MEst. However, all other reactions could also involve disproportionation by transfer of a β -hydrogen atom from the carbon-centered radical to the nitroxide to provide an alkene and a hydroxylamine. Some evidence for this process is available,^{13a,45,46} and therefore, we have determined the yields of disproportionation for several of the cross-reactions studied in this work.^{22,47} In comparison to coupling, they amount to only a few percent for Cum,²² PhEt, and PEst reacting with TEMPO and PhEt

(44) In ref 22, the temperature dependence for the reaction of Cum with TEMPO was given as $\log(k_c/\text{M}^{-1} \text{ s}^{-1}) = 8.4(1) - 3.7(3)/2.303RT$ (kJ mol⁻¹), that is, it was described by the Arrhenius equation, although the data leveled off at higher temperatures (cf. Figure 6).

(45) Li, I.; Howell, B. A.; Matyjaszewski, K.; Shigemoto, T.; Smith, P. B.; Priddy, D. B. *Macromolecules* **1995**, *28*, 6692. Moffat, K. A.; Hamer, G. K.; Georges, M. K. *Macromolecules* **1999**, *32*, 1004.

(46) Skene, W. G.; Scaiano, J. C.; Yap, G. P. A. *Macromolecules* **2000**, *33*, 3536.

(47) Ananchenko, G.; Fischer, H., to be published.

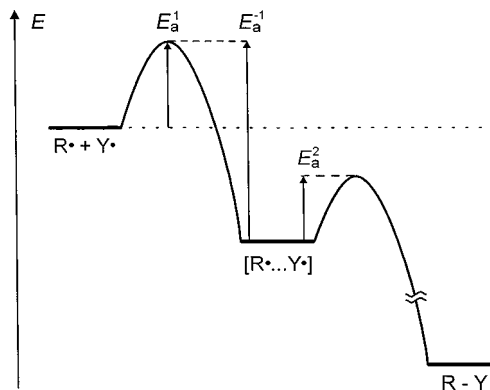


Figure 7. Energy-level diagram of a cross-coupling reaction with a transient intermediate.

reacting with SG1; that is, disproportionation is relatively unimportant in these cases and probably also for most of the other cases. However, for POH reacting with TEMPO, acetone and the hydroxylamine are the major products, and they account for >98% of the products.⁴⁷ Because POH is a very good electron donor, this reaction is presumably by electron transfer to the nitroxide, followed by transfer of the hydroxy proton; it is not a usual β -hydrogen atom transfer. We have noted above that in contrast to all other cases, POH reacts with TEMPO at a diffusion-controlled rate, and this seems to reflect the different mechanism. Hence, with the exception of this particular case, which is excluded from the further discussion, we assume that the cross-reaction is highly dominated by coupling.

In liquids, unusual temperature dependencies are known for several radical–radical reactions involving persistent radicals, such as self-reactions of acyl-, alkyl-, phenyl-, and dialkyl-nitroxides to a nitron and a hydroxylamine by disproportionation.^{48–52} The rate constants of these reactions are also much smaller than those that are diffusion-controlled ($4\text{--}7 \times 10^6 \text{ M}^{-1} \text{ s}^{-1}$) and depend little on temperature. Where the Arrhenius equation applies, the frequency factors are small, and the activation energies are close to zero. In some cases, the activation energies are even negative. For the explanation, unfavorable steric requirements for the transition geometry, that is, large entropic factors, have been addressed. However, in several self-reactions, intermediate dimer complexes were observed, and therefore, most of the discussions invoked the

(48) Adamic, K.; Bowman, D. F.; Gillan, T.; Ingold, K. U. *J. Am. Chem. Soc.* **1971**, *93*, 902.

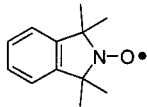
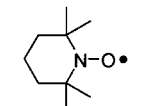
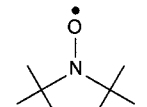
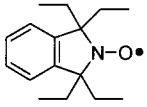
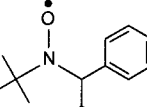
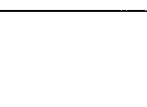
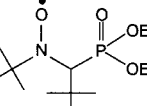
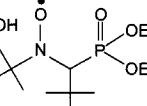
(49) Bowman, D. F.; Brokenshire, J. L.; Gillan, T.; Ingold, K. U. *J. Am. Chem. Soc.* **1971**, *93*, 6551.

(50) Bowman, D. F.; Gillan, T.; Ingold, K. U. *J. Am. Chem. Soc.* **1971**, *93*, 6555.

(51) Mendenhall, G. D.; Ingold, K. U. *J. Am. Chem. Soc.* **1973**, *95*, 6390.

(52) Griller, D.; Perkins, M. J. *J. Am. Chem. Soc.* **1980**, *102*, 1354.

Table 3. Rate Constants for the Cross-Termination of Nitroxide with Carbon-Centered Radicals

Nitroxide	C-Radical	Solv.	$k_{c,297}/$ $M^{-1}s^{-1}$	$k_{c,323}/$ $M^{-1}s^{-1}$	$k_{c,393}^a/$ $M^{-1}s^{-1}$	$k_{d,393}/$ s^{-1}
	Cum	tBB	$1.3(1) \cdot 10^8$	$1.4(1) \cdot 10^8$	$1.5 \cdot 10^8$	$4.1 \cdot 10^{-3,d}$
	MEst	ACN	$2.3(1) \cdot 10^9$			$8.1 \cdot 10^{-8}$
	POH	tBB	$1.4(1) \cdot 10^9$	$1.9(2) \cdot 10^9$	$2.9 \cdot 10^{9,b}$	
	CH	CHN	$9.6(2) \cdot 10^8$	$7.5(2) \cdot 10^8$		$2.1 \cdot 10^{-9}$
	PEst	ACN	$6.3(7) \cdot 10^8$	$6.5(6) \cdot 10^8$	$5.9 \cdot 10^8$	$2.2 \cdot 10^{-2}$
	Ben	tBB	$2.6(1) \cdot 10^8$	$3.1(1) \cdot 10^8$	$3.5 \cdot 10^8$	$1.1 \cdot 10^{-5}$
	PhEt	TMP	$4.3(1) \cdot 10^8$			
		tBB	$2.2(1) \cdot 10^8$	$2.3(1) \cdot 10^8$	$2.5 \cdot 10^8$	$5.2 \cdot 10^{-4}$
	Cum	tBB	$5.2(2) \cdot 10^7$	$5.7(3) \cdot 10^7$	$5.5 \cdot 10^7$	$8.5 \cdot 10^{-2}$
	Cl-Ben	tBB	$2.2(1) \cdot 10^8$	$2.4(1) \cdot 10^8$	$2.6 \cdot 10^8$	
	Ben	tBB	$1.8(1) \cdot 10^8$	$1.9(1) \cdot 10^8$	$2.1 \cdot 10^8$	$1.9 \cdot 10^{-4}$
	MeO-Ben	tBB	$9.7(1) \cdot 10^7$	$1.1(1) \cdot 10^8$	$1.2(1) \cdot 10^{8,c}$	
	PEst	ACN	$2.3(1) \cdot 10^8$	$2.3(1) \cdot 10^8$		$2.0 \cdot 10^{-1,d}$
	Cum	tBB	$1.1(1) \cdot 10^7$	$1.2(1) \cdot 10^7$	$9.4 \cdot 10^6$	$7.0 \cdot 10^{-1,d}$
	PEst	ACN	$3.9(2) \cdot 10^7$	$4.6(4) \cdot 10^7$		$8.3 \cdot 10^{-2,d}$
	PhEt	tBB	$8.0(2) \cdot 10^6$	$8.7(3) \cdot 10^6$	$8.2(2) \cdot 10^{6,c}$	$3.3 \cdot 10^{-2}$
	MEst	ACN	$8.0(2) \cdot 10^8$			$2.2 \cdot 10^{-6,d}$
	Ben	tBB	$1.1(1) \cdot 10^7$	$1.6(1) \cdot 10^7$	$2.8 \cdot 10^{7,b}$	$3.3 \cdot 10^{-4}$
	PhEt	tBB	$3.1(1) \cdot 10^6$	$3.7(2) \cdot 10^6$	$4.6 \cdot 10^6$	$5.3 \cdot 10^{-3}$
	PEst	ACN	$2.6(1) \cdot 10^6$	$1.8(1) \cdot 10^6$	$1.1 \cdot 10^6$	$5.0 \cdot 10^{-2}$
	Cum	tBB	$\leq 2 \cdot 10^{5,e}$			1.7^d
	PhEt	tBB	$3.0(1) \cdot 10^6$	$4.0(2) \cdot 10^6$	$8.8 \cdot 10^{6,b}$	$1.8 \cdot 10^{-2}$

^a Calculated using eq 9 and the parameters of Table 4. ^b Calculated using the Arrhenius equation and the parameters of Table 4. ^c Measured at 373 K. ^d Estimated; see ref 20. ^e Upper limit.

existence of an intermediate. This was also implied for the slow combination of 2-oxomorpholinyl radicals.⁵³

To analyze our findings in the same way, we start from the schematic energy profile of Figure 7. Here, the intermediate is

Table 4. Activation Parameters for the Cross-Coupling of Nitroxide with Carbon-Centered Radicals

nitroxide	C radical	solv	$E_a^1/\text{kJ mol}^{-1}$	$\log(A_1/M^{-1} \text{s}^{-1})$	$E_a^1 - E_a^2/\text{kJ mol}^{-1}$	$\log(A_{-1}/A_2)$	data points
TMIO	Cum	tBB	17.5(1)	11.6	23.0(20)	4.2(5)	8
TEMPO	POH	tBB	7.7(9) ^a		10.5(2) ^a		8
	PEst	ACN	14.1(2)	11.5	18.4(29)	3.3(18)	8
	Ben	tBB	15.6(3)	11.6	16.7(13)	3.2(2)	11
	PhEt	tBB	15.5(2)	11.6	17.1(9)	3.4(1)	13
	Cum	tBB	18.2(2)	11.6	19.8(11)	4.1(2)	7
DBNO	Cl-Ben	tBB	15.4(11)	11.6	16.3(32)	3.3(5)	6
	Ben	tBB	15.2(6)	11.6	15.4(16)	3.3(5)	12
TEDIO	Cum	tBB	20.2(6)	11.6	23.4(24)	5.1(5)	8
SG1	Ben	tBB	8.7(5) ^b		8.6(1) ^b		7
	PEst	AN	20.3(7)	11.5	29.0(16)	6.6(2)	8
	PhEt	tBB	23.5(10)	11.6	17.9(22)	4.1(3)	8
HO-SG1	PhEt	tBB	10.3(5) ^b		8.3(1) ^b		10

^a $E_a/\text{kcal mol}^{-1} = E_a/\text{kJ mol}^{-1}/4.185$. ^b Arrhenius parameters.

formed with rate constant k_1 and decays with rate constants k_{-1} to the parent free radicals and with k_2 to the final product. Assumption of a short lifetime and a steady state for the intermediate casts the overall reaction rate constant into the form

$$k_c = \frac{k_1 k_2}{k_{-1} + k_2} \quad (8)$$

If all individual rate constants obey the Arrhenius equation, this is equal to

$$k_c(T) = \frac{A_1 e^{-\frac{E_a^1}{RT}}}{1 + \frac{A_{-1}}{A_2} e^{-\frac{E_a^{-1} - E_a^2}{RT}}} \quad (9)$$

Empirically, very good fits of eq 9 to the experimental data were obtained. To avoid too many free parameters, we assumed that k_1 is diffusion-controlled and set A_1 equal to the frequency factor of $2k_t$ in the respective solvent (Table 2). The residual parameters E_a^1 , E_a^{-1} , and A_{-1}/A_2 resulting from the fits are given in Table 4, and temperature dependencies reproduced using these are shown in Figures 5 and 6. If the formation of the intermediate is diffusion-controlled, the activation energies E_a^1 should be similar to those given in Table 2. They are slightly larger (Table 4) but of similar magnitude, which supports the approach. Except for the reaction of PhEt with SG1, the difference $E_a^{-1} - E_a^2$ is larger than E_a^1 . This relation was used to draw Figure 7, and it is a precondition for a reaction via an intermediate that can yield a negative temperature dependence of the rate constant.⁵⁴

The parameter (A_{-1}/A_2) is in the range of 10^3 – 10^6 , and it increases with decreasing rate constant (Table 4). If k_{-1} represents a simple fission of a loose complex with little entropy change, A_{-1} should be about 10^{13} s^{-1} , and then A_2 would range from 10^7 to 10^{10} s^{-1} . Hence, the conversion of the intermediate to the products has a very low frequency factor, and this lowers the overall rate constant. Obviously, this reaction must be strongly hindered for entropic reasons. Actually, in the series Ben, PhEt, and Cum reacting with TEMPO, the ratio A_{-1}/A_2 increases regularly. It is larger for Cum reacting with TEDIO

and particularly large for PEst with SG1 (Table 4). Because, from the radical structures (Schemes 1, 2), the geometric constraints may increase in this series, an increasingly negative activation entropy for the product formation from the intermediate seems not unreasonable.

This interpretation is in keeping with the earlier discussions of unusual temperature dependencies of self-terminations of persistent radicals^{48–52} and other processes,^{55–57} but we have not found any direct or indirect evidence for the possible intermediate. The reverse alkoxyamine cleavage reaction shows a normal temperature dependence with a large positive activation energy.^{20–22} Kinetic absorption spectroscopy did not reveal additional absorbances on the 100-ns-or-longer time scale. In addition, we searched for a potential intermediate by B3LYP/6-31G* calculations. In these, the C–O bond of the model compound *O*-benzyl-*N,N*-dimethylhydroxylamine was extended by 20 steps of 0.1 Å. For each step, the structure was optimized except for the phenyl ring, which was fixed to a planar geometry with bond angles of 120° but variable though uniform C–C and C–H bond lengths. With increasing C–O bond length, the energy increases to a maximum of 154 kJ mol⁻¹ (36.8 kcal mol⁻¹) and decreases to a limiting value of 149 kJ mol⁻¹ (35.6 kcal mol⁻¹) thereafter. This is in reasonable agreement with known activation energies and bond dissociation energies for the cleavage of related hydroxylamines.²⁰ However, at no distance was there found an additional energy minimum indicating a possible intermediate. Also, we noticed that the intermediate could have some charge-transfer character, because some of our radicals (e.g., Ben, PhEt and Cum) have low ionization energies, and because the electron-transfer reaction of POH with TEMPO would be in keeping with an intermediate charge-transfer complex. If this would hold, the cross-reaction rates should be influenced by the donor properties of the carbon-centered radical, that is, they should increase in the series Cl–Ben, Ben, and MeO–Ben. However, Table 3 reveals no significant rate differences for the reaction of these radicals with TEMPO, so that at least a highly polar intermediate can be excluded.

Although all of this does not rule out the two-step process with a short-lived intermediate, the weak, curved, or even negative temperature dependence of the cross-reaction constants does not prove it either. In fact, it is also compatible with a nearly barrierless single-step reaction. In the gas phase, numer-

(53) Olson, J. B.; Koch, T. H. *J. Am. Chem. Soc.* **1986**, *108*, 756.

(54) Mozurkewich, M.; Benson, S. W. *J. Phys. Chem.* **1984**, *106*, 6429. Mozurkewich, M.; Lamb, J. J.; Benson, S. W. *J. Phys. Chem.* **1984**, *106*, 6435. Lamb, J. J.; Mozurkewich, M.; Benson, S. W. *J. Phys. Chem.* **1984**, *106*, 6441.

(55) Kiselev, V. D.; Miller, J. G. *J. Am. Chem. Soc.* **1975**, *97*, 4036.

(56) Turro, N. J.; Lehr, G. F.; Butcher, J. A.; Moss, R. A.; Guo, W. J. *Am. Chem. Soc.* **1982**, *104*, 1754.

(57) Reitstöben, B.; Parker, V. D. *J. Am. Chem. Soc.* **1990**, *112*, 4968.

ous electronically barrierless radical–radical reactions exhibit weak, curved, or negative temperature dependencies and have been covered by appropriate theories.⁵⁸ In loose terms of the dynamical theories, a rate constant is governed by the number of quantum states available to the system at the transition geometry. For a single step coupling reaction of polyatomic species without electronic barrier, this number is smaller at smaller, rather than at larger, reactant distances, because the energy spacings of the internal degrees of freedom increase with decreasing distance; for example, free rotations become restricted. The reduced number determines the location of the transition state and causes a dynamical bottleneck.⁵⁹ In addition, the difference of states available at large and small distances increases with increasing temperature. This shifts the transition state to smaller distances and decreases the rate constants at higher temperatures. In terms of the Eyring equation, the motional restrictions upon approach of the transition state mean negative contributions to the activation entropy, and therefore, barrierless reactions may show large negative activation entropies. In addition, as seen below, the shift of the transition geometry may even cause negative activation energies.

On the basis of quantum chemical calculations, a pictorial description of such entropy-controlled single-step reactions has first been offered by Houk and co-workers.^{60,61} It has been used in discussions of rates of chlorocarbene additions to alkenes,^{60–62} of a radical dimerization,⁵³ and of electron-transfer reactions.⁶³ To apply it to the present case, we first consider the reverse reaction of the coupling, namely, the cleavage of alkoxyamines. The cleavage rate constants and their temperature dependence have been studied extensively.^{12–22} They reveal characteristic features of the transition state that is the same for the coupling. First, the cleavage activation energies range from 80 kJ mol⁻¹ (19 kcal mol⁻¹) to about 180 kJ mol⁻¹ (43 kcal mol⁻¹) and depend on the nitroxide and the leaving radical. They are governed by the stability of the latter and by electronic and steric effects of both the nitroxide and the radical substituents. Moreover, they are close to the C–O bond-dissociation energies calculated using advanced methods,^{19,20} and our B3LYP calculation provides the same result. This means that the coupling reaction can have only a very small intrinsic electronic barrier. Second, the frequency factors of the cleavage are in the range of 10¹³–10¹⁵ s⁻¹. A clear variation with the alkoxyamine structure has not yet been found, and the data cluster at $\sim A_d = 2.6 \times 10^{14}$ s⁻¹. Such frequency factors are small for a fragmentation into two large groups where $A > 10^{15}$ s⁻¹ is expected.⁶⁴ Hence, the cleavage has a fairly early transition state with little elongation of the C–O-bond. At the transition geometry, only a minor part of the total reaction entropy has been gained, although the total reaction enthalpy has been nearly consumed. Conversely, the coupling occurs at short distance and should show a large negative activation entropy.

Following Houk,^{60,61} these considerations allow the construction of a schematic diagram for the evolution of the energies ΔH , $-T\Delta S$, and $\Delta G = \Delta H - T\Delta S$ during the cleavage of an

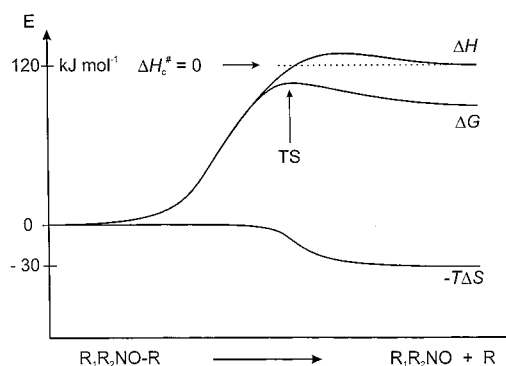


Figure 8. Schematic variations of ΔH , $-T\Delta S$ and ΔG along the reaction coordinate for a typical nitroxide/alkyl radical pair. TS denotes the position of the transition state.

alkoxyamine and during the reverse coupling. The energies of the alkoxyamine are taken as origin. To draw a realistic diagram, we assume an average temperature independent reaction enthalpy of 120 kJ mol⁻¹ (28.7 kcal mol⁻¹) for the cleavage. For the reverse coupling, we adopted a small barrier of about 10 kJ mol⁻¹ (2.4 kcal mol⁻¹). This may be diffusional or intrinsic. The total reaction entropy is also assumed to be temperature independent. It is estimated from the average frequency factor of the cleavage ($A_d = 2.6 \times 10^{14}$ s⁻¹) and from the frequency factors of the two coupling reactions Ben + SG1 and PhEt + HO – SG1 ($A_c = 3.2 \times 10^8$ M⁻¹ s⁻¹, Table 4), which show a normal Arrhenius behavior as $\Delta S = 100$ J mol⁻¹K⁻¹ (24 cal mol⁻¹K⁻¹) and $T\Delta S = 30$ kJ mol⁻¹ (7.2 kcal mol⁻¹) at room temperature. The activation parameters of the cleavage showed that on the dissociative approach of the transition state, nearly the total reaction enthalpy is needed, but only about 30 J mol⁻¹K⁻¹ (24 cal mol⁻¹K⁻¹) of the reaction entropy is gained. Figure 8 reveals that for these energetic conditions, the transition state (the maximum of ΔG) is markedly shifted from the maximum of ΔH to lower C–O bond distances by the entropy term. With increasing temperature, this shift should increase, because $T\Delta S$ increases.

For the cleavage reaction, the activation energy $E_{a,d} = \Delta H_d^\ddagger + RT$ is governed by the large enthalpy term. The activation entropy is small so that possible variations with substituents are of minor influence. Hence, the cleavage rate constants should exhibit a normal Arrhenius-type temperature dependence as it is observed. On the other hand, for the coupling reaction with its small intrinsic enthalpic barrier, the situation is different. At the transition geometry, ΔH_c^\ddagger should be smaller than the small intrinsic or diffusional barrier, and Figure 8 shows that ΔH_c^\ddagger may be close to zero, or even negative. Because $E_{a,c} = \Delta H_c^\ddagger + RT$ for a liquid-phase reaction, small positive, zero, or even negative activation energies may result. With increasing temperature, the maximum of ΔG will shift to lower values of ΔH_c^\ddagger . Hence, if ΔH_c^\ddagger decreases more than RT increases, the activation energy will become more negative with increasing temperature.

Further extending Houk's arguments,^{60,61} we note in addition that extent of entropy control should depend on the alkoxyamine bond dissociation energy, because the descent of the enthalpy in the transition region will flatten out with decreasing exothermicity of the coupling. This increases the influence of the entropy term, and therefore, in a series of cross-couplings with diminishing exothermicity but equal negative activation entropies, the rate constants should decrease.

As mentioned above, in gross terms, the rate constants of the cross-reaction are small for fast alkoxyamine decays and vice versa. Because the alkoxyamine decays are governed by

(58) Truhlar, D. G.; Garrett, B. C.; Klippenstein, S. J. *J. Phys. Chem.* **1996**, *100*, 12771.

(59) Wardlaw, D. M.; Marcus, R. A. *J. Phys. Chem.* **1986**, *90*, 5383.

(60) Houk, K. N.; Rondan, N. G.; Mareda, J. *Tetrahedron* **1985**, *41*, 1555.

(61) Houk, K. N.; Rondan, N. G. *J. Am. Chem. Soc.* **1984**, *106*, 4291. Keating, A. E.; Merrigan, S. R.; Singleton, D. A.; Houk, K. N. *J. Am. Chem. Soc.* **1999**, *121*, 3933.

(62) Moss, R. A.; Lawrynowicz, W.; Turro, N. J.; Gould, I. R.; Cha, Y. *J. Am. Chem. Soc.* **1986**, *108*, 7028.

(63) Frank, R.; Greiner, G.; Rau, H. *Phys. Chem. Chem. Phys.* **1999**, *1*, 3481.

(64) Benson, S. W. *Thermochemical Kinetics*; Wiley: New York, 1968. Rüdhardt, C.; Beckhaus, H.-D. *Angew. Chem.* **1980**, *92*, 417.

the activation energies, and these are close to the bond dissociation energy, fast decays mean small exothermicities of the cross-reaction, and hence, the trend agrees with the prediction. In particular, for the reactions of the cumyl radical with nitroxides, the activation energies of the cleavage decrease in the order TMIO (118.9 kJ mol⁻¹) > TEMPO (115.7 kJ mol⁻¹) > TEDIO (≈109.4 kJ mol⁻¹). The influence of the entropy term should increase in that order, and in fact, Figure 6 shows that the deviations from the Arrhenius behavior increase and the temperature maximum of the rate constant shifts to lower values. Also, the rate constants decrease in the series. For the cleavage reactions involving SG1, the activation energies are 134.6 kJ mol⁻¹ (32.2 kcal mol⁻¹) for Ben, 124.5 kJ mol⁻¹ (29.7 kcal mol⁻¹) for PhEt, and ≈111.6 kJ mol⁻¹ (26.7 kcal mol⁻¹) for PEst. Again and as expected, the deviations from the Arrhenius behavior increase in this order (Figure 5). For Cum dissociating from SG1, a very low activation energy of 107 kJ mol⁻¹ (25.6 kcal mol⁻¹) has been estimated,²⁰ and this agrees with the unmeasurably low cross-coupling rate constant.

Whereas these results are nicely explained by the decreasing alkoxyamine bond dissociation energy alone, which favors the expression of the entropy term, and need no variation of the latter, there is no unique correlation between the cross-coupling rate constants and the rate constants for the cleavage. This points to additional substituent effects on the individual activation entropies. For instance, in comparison to TIPNO and SG1, the cross-reactions with TEMPO, DBNO, and TEDIO are faster than expected from the rates of the corresponding alkoxyamine cleavage. Furthermore, there is a much larger dependence of the cross-coupling constants on the structure of the carbon-centered radical for SG1 than for TEMPO, although the cleavage rates and their activation energies vary similarly with substitution in the two series. Obviously, the activation entropy for cross-coupling is considerably more negative for reactions involving SG1 and TIPNO than for TEMPO, DBNO, and TEDIO.

In total, Houk's model^{60,61} gives a satisfactory explanation for the trend of a grossly reverse ordering of the alkoxyamine cleavage and the corresponding cross-coupling constants. Therefore, it is preferred as the explanation for the unusual temperature dependencies of the cross-coupling rates. The same principle may well apply also for other cross-reactions involving persistent radicals, but the model calls for support by high-level calculations of the transition structures, enthalpies, and entropies. These are still difficult for our rather large systems. The model also predicts that a non-Arrhenius behavior should always appear for radical couplings with intrinsically small barriers, if the reverse cleavage processes have small barriers, and if there are large constraints imposed on the transition state by unfavorable

radical structures. It is known that many transient radicals self-terminate with diffusion controlled rates, and additional examples have been given in Table 2. In these cases, the intrinsic barriers to coupling or disproportionation are small, but the reverse processes have large barriers and the steric constraints are minor. Hence, for usual radical couplings leading to strongly bonded systems, the deviations from the Arrhenius behavior should be small and eventually be observable only at high temperatures.^{60,61}

In nitroxide-mediated living radical polymerizations, the carbon-centered radicals are polymeric species with many monomer units. In earlier comparisons,^{7,8,20} the rate constants of their coupling with nitroxides and of the corresponding alkoxyamine cleavage were found to be similar to those of the low-molecular-weight models considered here. Hence, at least the same trends should hold for low-molecular-weight and polymeric systems. Of practical importance are the now confirmed small temperature dependence of the cross-coupling constants which differ, at most, by a factor of 2 between room temperature and 120 °C. This facilitates extrapolations and eliminates the need for extensive series of experiments at different temperatures. Additionally, for the most simple mechanism of living polymerizations^{7,8} involving only the reversible cleavage of the alkoxyamine, addition of monomer, and irreversible termination of the carbon-centered radicals, the cleavage and cross-coupling constants k_d and k_c strongly influence the course of the process. Thus, a large equilibrium constant of the reversible cleavage k_d/k_c leads to short polymerization times, and a large product $k_d k_c$ provides small polydispersities. Moreover, a large k_d is required to obtain a linear increase of the degree of polymerization with increasing conversion already at low conversions. Table 3 shows that, for the same carbon-centered radical, k_d is considerably smaller for TEMPO and TMIO than for DBNO, TEDIO, TIPNO, and SG1. The cross-coupling constants are much larger for TMIO, TEMPO, and DBNO than they are for TIPNO and SG1. Hence, in terms of the polymerization rate, TIPNO and SG1 offer distinct advantages that are confirmed by practice.^{11,19,65}

Acknowledgment. We thank the Swiss National Foundation for Scientific Research for financial support, Mrs. I. Verhoolen for the syntheses of ketones and several alkoxyamines, P. Tordo (Marseille) and Ciba SC (Basel) for nitroxides and alkoxyamines, and G. Ananchenko and M. Weber for mechanistic studies.

JA0036460

(65) Benoit, D.; Chaplinski, V.; Braslau, R.; Hawker, C. J. *J. Am. Chem. Soc.* **1999**, *121*, 3904.